

## Photodegradation of surfactants with TiO<sub>2</sub> semiconductor for the environmental wastewater treatment

HISAO HIDAKA

Frontier Research Center for the Earth Environmental Center, Department of Chemistry, Meisei University, 2-1-1 Hodokubo, Hino, Tokyo 191-0042, Japan

**Abstract.** Surfactants were photodegraded in TiO<sub>2</sub> suspensions under UV irradiation. The photodegradation mechanism of chemical structures of surfactants, the time scale in the photooxidative decomposition and the intermediate products were investigated. Various surfactants are widely used in domestic and industrial fields. However, they are not easily biodegraded through bacteria and are accumulated in the nature of alkylphenylpolyoxyethylene which generates toxic intermediates of alkylphenol derivatives which are immiscible in water during biodegradation. Since the cationic surfactant exhibits antimicrobial activity, the biodegradation is poor. The other strategy of this study is also a harvest of photocurrent during the transformation process.

**Keywords.** Surfactants; photodegradation; TiO<sub>2</sub> electrode assembly; oxyethylene group.

### 1. Introduction

The photooxidation of organic substances catalyzed with TiO<sub>2</sub> semiconductor was first published by Carry in 1976 who dealt with the photodecomposition of chlorobiphenyl compound in heterogeneous TiO<sub>2</sub> particle dispersion. The fundamental and applied researches for the environmental wastewater treatment have been actively advanced globally to solve severe aquatic and air contamination. In particular, the photodegradation of carcinogenic chloroorganics of trichloroethylene, chlorophenol etc., phosphorus-, nitrogen- or sulphur-containing agrochemicals such as pesticides and herbicides, cyanide compounds and polymers of polyvinylalcohol, polyethylene-glycol etc. has been extensively reported by many researchers.

The photocatalytic degradation with TiO<sub>2</sub> catalyst is one of the most promising procedures. All kinds of surfactants can be mineralized to CO<sub>2</sub>, H<sub>2</sub>O and other inorganic ions and organic acids in a short time without formation of toxic intermediates, irrespective of the structures of surfactants. Since an amphiphilic surfactant contains both hydrophobic alkyl group and hydrophilic functional group in one molecule, the details of decomposition mechanisms and adsorption behaviours on the surface can be informed at a molecular level.

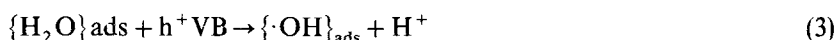
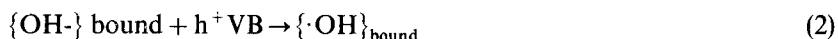
In this paper, we describe the recent experiment on the photomineralization or phototransformation for functional moieties of sulphate, phosphate and quaternary ammonium group and hydrocarbons of an alkyl chain and an ethoxyl group in TiO<sub>2</sub> dispersion systems. Further, the TiO<sub>2</sub>-fixation procedure on glass fibres, glass beads, ceramic tiles and honeycombs is studied from the viewpoint of an industrial application for continuous and large scale treatments. The fixation procedures need no operation

for removal. The photooxidative activity still maintains even in repeated runs (turn-over). The electrochemical decomposition of organic pollutants containing surfactants such as the big  $\text{TiO}_2$  semiconductor of TCO (transparent conductive oxide) electrode assemblies has been carried out by us<sup>1</sup>. The other strategy of this study is also a harvest of photocurrent during the transformation process. We introduce the recent results later in section 7.

## 2. Photodegradation principle of organics catalyzed by $\text{TiO}_2$ semiconductor

The photochemical and physical kinetics on photoexcitation processes in semiconductor  $\text{TiO}_2$  particles are shown in figure 1.

$\text{TiO}_2$  is a *n*-type semiconductor having a bandgap of 3.2 eV. Therefore, the charge separation by UV illumination below 387 nm occurs to generate electron holes ( $h^+$ ) in a valence band and electrons in a conduction band respectively (1). The holes capture the electrons from  $\text{H}_2\text{O}$  molecules adsorbed and/or hydroxyl groups bound on the  $\text{TiO}_2$  particle surface (2 and 3). Concomitantly, the dissolved oxygen accepts the electron from the conduction band to form  $\cdot\text{O}_2^-$ . This radical reacts with protons in aqueous solution to generate  $\cdot\text{OOH}$  radicals (4 and 5). The highly reactive radicals were confirmed by spin-trapping ESR measurements using DMPO reagent.



The actively oxidative radicals of  $\cdot\text{OH}$  or  $\cdot\text{OOH}$  are attacked to the organics adsorbed or assessed on  $\text{TiO}_2$  surface and the organics are photooxidized. The direct oxidation of

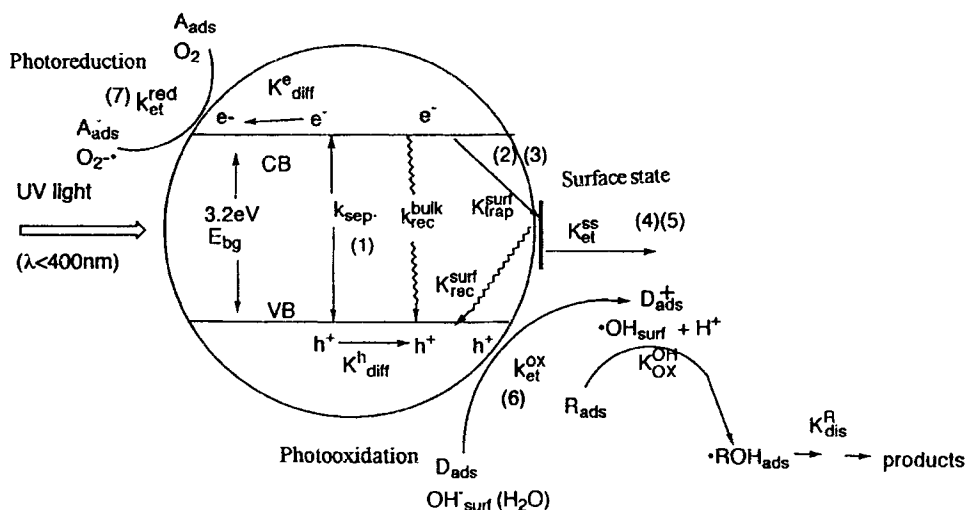


Figure 1. The photophysical and photochemical processes in a semiconductor.

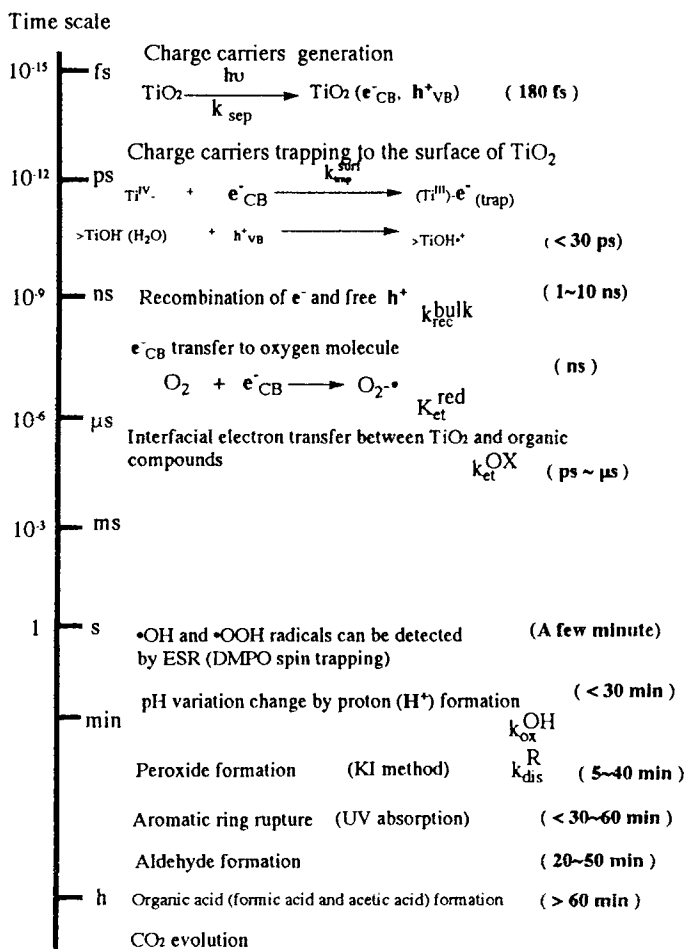


Figure 2. Time scale of photocatalytic oxidation.

the organics with the holes in the valence band takes place in a parallel manner. Particularly, the  $\pi$ -electrons in an aromatic ring capture the electrons by the hole to form cationic radicals.

### 3. Time scale in the photooxidative decomposition

The mechanistic details on the charge separation rate in semiconductor particles and electron transfer rate have been studied by laser flash photolysis. The time scale on the photooxidative degradation process for an organic substance is summarized in figure 2.

When TiO<sub>2</sub> particles are irradiated by ultraviolet (UV) light, electrons and holes are formed within an ultrafast rate below 180 fs in a crystal, followed by capturing the electrons at the defecting moiety in a lattice on TiO<sub>2</sub> surface. The electron holes react with the hydroxyl groups (and/or bound water) combined with TiO<sub>2</sub> surface at the rate within 30 ps. The transfer rate of electrons in a conduction band to O<sub>2</sub> molecules is relatively slow in nanosecond order as Gerisher *et al* has postulated<sup>2</sup>.

This step is a rate-determining step in a photocatalytic reaction. Consequently, no photodecomposition proceeds effectively in the absence of oxygen molecules. Many charge-carriers ( $e^-$  and  $h^+$ ) formed by photoexcitation within  $1 \sim 10$  ns disappear by the recombination of  $e^-$  and  $h^+$  in a  $TiO_2$  bulk and then the electron transfer occurs between an organic compound and  $TiO_2$  particles.

Although the rate is dependent on the kind of an organic compound, this process proceeds within ps to ms. Formation of  $\cdot OH$  or  $\cdot OOH$  radicals is detected within 30 min and simultaneously protons are generated by photolysis of  $H_2O$ . Totally, the reaction solution becomes acidic. The hydrocarbon moiety in a surfactant is attacked

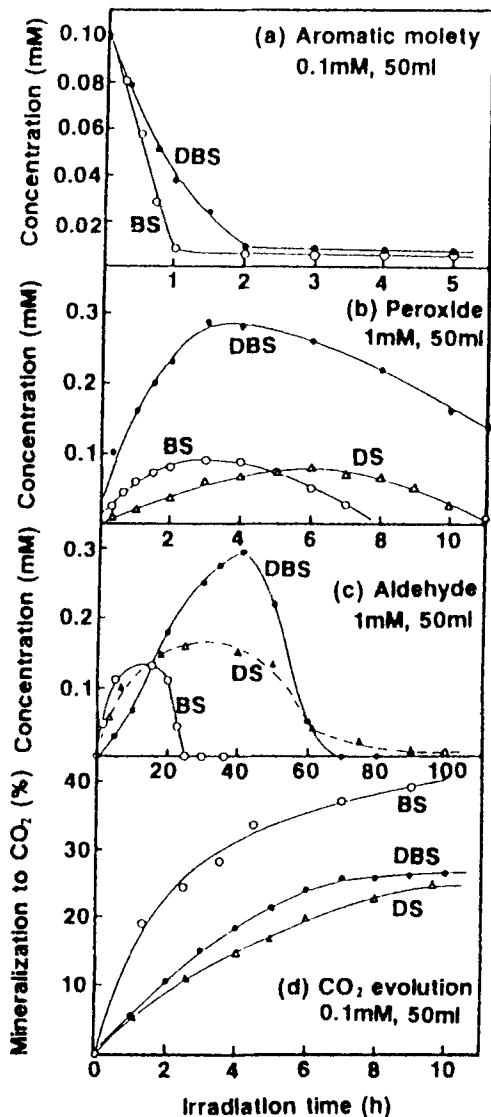


**Figure 3.** Photodegradation of anionic DBS and its reference substances DS and BS in air-equilibrated aqueous suspension (50 ml, 1 or 0.1 mM) of  $TiO_2$  (100 mg) under Hg-lamp irradiation.

by actively oxidative species to prepare a hydroxylated compound and a hydroxy-peroxide derivative (confirmed by the KI method). Subsequently, these compounds are mineralized to  $\text{CO}_2$  via aldehyde or carboxylic acid intermediates by photooxidation and/or autooxidation. A hetero atom moiety is photoconverted to inorganic ions. An aromatic moiety such as benzene<sup>-</sup> or pyridine<sup>-</sup> ring is easily cleaved. Formation of peroxide, the ring-opening of benzene group, formation of aldehyde and  $\text{CO}_2$  evolution in the photodegradation of DBS (sodium dodecylbenzene sulphonate) are shown in figure 3.

The time required for secondary oxidation on  $\text{TiO}_2$  surface or in a bulk solution occurs in the order of several minutes to hours.

#### 4. Adsorption and photodecomposition rate

The photodegradation rate in heterogeneous  $\text{TiO}_2$  dispersion follows Langmuir–Hinshelwood equation (L–H plot) using a monomolecular layer reaction on a solid catalyst.

$$r_{\text{initial}} = kK/(1 + KC) \quad (6)$$

$$1/r = 1/kK \times 1/c + 1/k, \quad (7)$$

where  $k$  is a reaction kinetic constant,  $K$  an adsorption equilibrium constant, and  $C$  an initial concentration. The plot of the reciprocal kinetic constant against the reciprocal concentration exhibits a linear relationship. The intercept is  $k^{-1}$  and the slope is  $kK^{-1}$ . The decomposition reaction of a surfactant is very complicated because of many competitive reactions. Therefore, the definition of an apparent reaction rate constant  $k$  is difficult.

Figure 4 shows the L–H plot for the photodecomposition of anionic DBS and cationic BDDAC (benzyltetradecyl dimethyl ammonium chloride). The adsorption

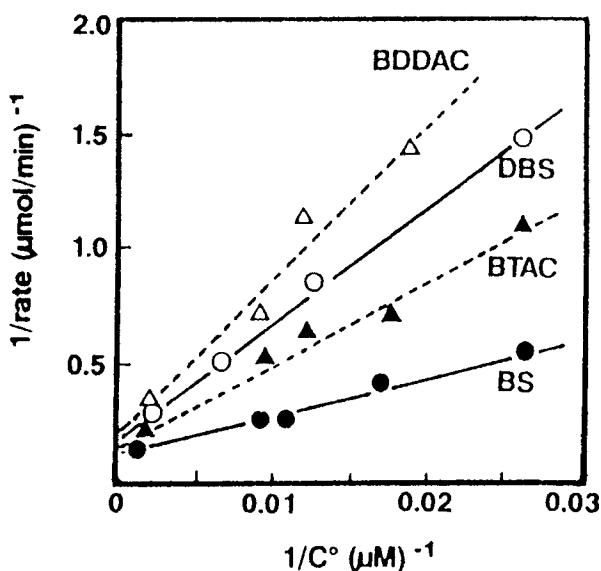


**Figure 4.** Langmuir–Hinshelwood plot of reciprocal initial rate against reciprocal initial concentration for DBS, BDDAC, BS, and BTAC.

equilibrium constant calculated from the plot is determined to be almost  $5.9 \text{ mM} \pm 0.03 \text{ mM/min}$ . On the other hand, the rate constant is dependent on the chemical structure of a substrate. The lifetime of  $\cdot\text{OH}$  or  $\cdot\text{OOH}$  radicals generated on  $\text{TiO}_2$  surface is short that the adsorption of a substrate on  $\text{TiO}_2$  surface is remarkably affected on the decomposition rate.  $\text{TiO}_2$  has an amphoteric compound having the isoelectric point  $\text{pH}_{\text{pzc}} = 6.2$ . The surface potential is a positive charge in acidic range, while it is a negative charge in alkaline range. Under UV irradiation, the degraded solution become acidic according to (3) in section 2 and the  $\text{TiO}_2$  surface is charged positively. Therefore, an anionic surfactant is adsorbed electrostatically on  $\text{TiO}_2$  surface and the photodegradation rate is accelerated. On the other hand, that of a cationic surfactant is slower because of electrostatic repulsion.

## 5. Experimental procedures (photodegradation in a heterogeneous dispersion)

In a batch system, a surfactant solution (50 ml) with anatase  $\text{TiO}_2$  particles (100 mg Degussa P-25, average particle size 30 nm) was placed in 70 ml reaction vessel and was illuminated with a mercury lamp ( $\lambda > 330 \text{ nm}$ , Toshiba SHL-1002A, 75 W) and stirred magnetically. After illumination, the degraded solution was centrifuged and filtered with a millipore filter ( $0.22 \mu\text{m}$ ) to remove  $\text{TiO}_2$  particles.

## 6. Degradation mechanism for the chemical structures of surfactants

### 6.1 Nitrogen-containing surfactants

There are few papers on the photocatalytic oxidation of nitrogen-containing compounds. Although the photodecomposition for agrochemicals of a herbicide or a pesticide containing the structures of benzamide, pyridine, triazine were published, the photoconversion of a nitrogen moiety has received much attention. Matthews *et al* 1991 reported the photooxidation of various nitrogen-containing organics<sup>3</sup>. However, the relationship between the structure of nitrogen and the ratio of  $\text{NH}_4^+$  ion/ $\text{NO}_3^-$  ion and the formation processes have not been revealed. The concomitant formation of  $\text{NH}_4^+$  ion  $\text{NO}_3^-$  ion on nitrogen-containing substances in the photocatalytic oxidation processes is very interesting.

Among surfactants, most of them have cationic surfactant having strong antibacterial activity, a nonionic one and an amphoteric one having non-irritation to skin which contain quaternary ammonium nitrogen ( $-\overset{|}{\text{N}}-$ ), secondary amine ( $-\text{NH}-$ ), tertiary amine ( $\overset{|}{\text{N}}\langle$ ) and peptide ( $-\text{CONH}-$ ) in their chemical structures. We discuss the decomposition mechanism for the nitrogen moieties of the following surfactants<sup>4</sup>: cationic BTDAC and dodecyl pyridinium chloride (DPC), nonionic dodecanoyl-N-(2-hydroxyethyl) amide (N-DHA) and dodecanoyl-N,N-bis(2-hydroxyethyl) amide (N, N-DHA), amphoteric dodecyl- $\beta$ -alanine ( $\text{C}_{12}$ - $\beta$ -Ala), N-(2-hydroxydodecyl)-N-(2-hydroxyethyl)- $\beta$ -alanine ( $\text{C}_{12}$ -HAA), N-dodecylamidopropyl-,N,N-dimethylammonium acetate ( $\text{C}_{12}$ -amidobetaine) as shown in figure 5.

A surfactant solution (0.1 mM, 50 ml) was photodegraded according to the method as mentioned in section 5. The nitrogen moieties in a nitrogen-containing surfactant was photoconverted to  $\text{NH}_4^+$  ion and  $\text{NO}_3^-$  ion, but not to inorganic compounds of  $\text{N}_2$  and  $\text{NO}_2$  gas.

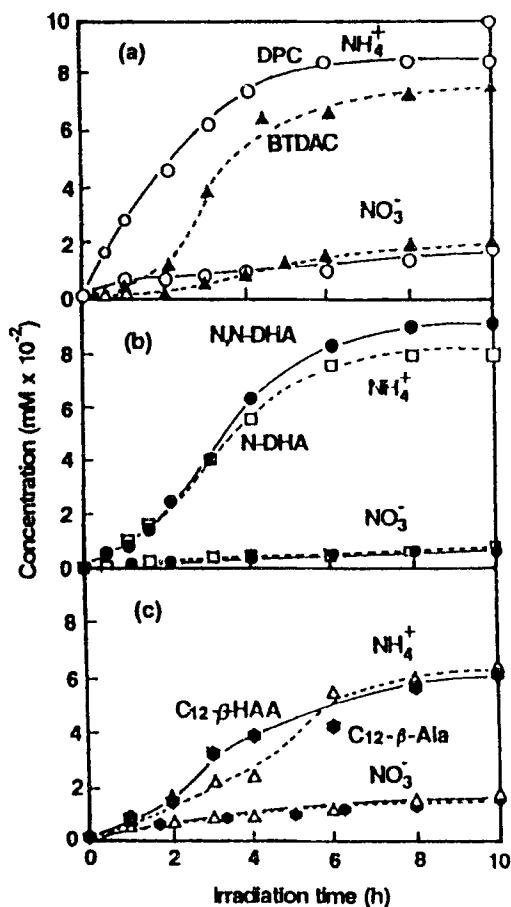


**Figure 5.** Formation of ammonium and nitrate ions in the photomineralization of (a)  $\circ$ , DPC and  $\blacktriangle$ , BTDAC; (b)  $\square$ , N-DHA and  $\bullet$ , N,N-DHA; (c)  $\Delta$ ,  $\text{C}_{12}$ - $\beta$ -Ala and  $\star$ ,  $\text{C}_{12}$ - $\beta$ -HAA as a function of irradiation time.

$\text{NH}_4^+$  ion was mainly formed in comparison with the formation ratio of  $\text{NH}_4^+/\text{NO}_3^-$ . The formation rate is dependent on the chemical structure. On the other hand, the amount of  $\text{NO}_3^-$  ion was almost 0.01 mM after irradiation of 8 h irrespective of the chemical structure. The decomposition of DPC easily caused the ring-opening of pyridine moiety which was confirmed by UV spectroscopy. The rate of  $\text{NH}_4^+$  ion formation is very fast. The decomposition rate of amphoteric surfactants is slower than that of cationic and nonionic surfactants. Since an amphoteric one has both negative and positive charges it is the reason attributed to the unstable adsorption on  $\text{TiO}_2$  surface. The identification of the intermediates in the photodegradation of amphoteric  $\text{C}_{12}$ -amidobetaine was done by GC-MS and NMR techniques. The C-N bond in  $\text{C}_{12}$ -amidobetaine was cleaved as an initial step. The intermediates of dodecanoamide, tertiary amine and/or quaternary ammonium were produced subsequently. The intermediate of amide is easily hydrolyzed to form  $\text{NH}_4^+$  ions. By contrast, the intermediates of tertiary amine or quaternary ammonium were attacked by  $\cdot\text{OH}$  and/or  $\cdot\text{OOH}$  radicals to convert finally to  $\text{NH}_4^+$  and  $\text{NO}_3^-$  ions. The decomposition of nitrogen

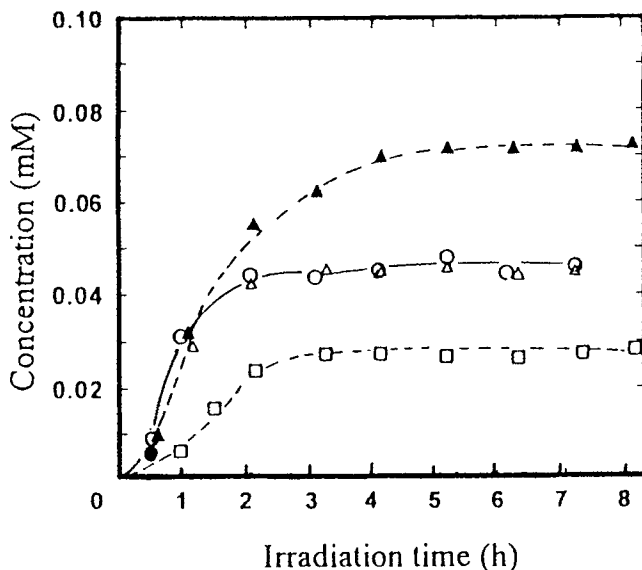


**Figure 6.**  $\text{SO}_4^{2-}$  ion formation from the degradation of DBS;  $\circ$ , BS;  $\Delta$ , SDS;  $\blacktriangle$ , and TPA;  $\square$ , in the presence of  $\text{TiO}_2$  catalyst.

moieties in surfactants is slower in the following order: pyridine ring > secondary amine > tertiary amine > peptide > quaternary ammonium.

To reveal the formation mechanism of  $\text{NH}_4^+$  and  $\text{NO}_3^-$  ions, various model compounds of alkylamide and hydroxy succinoimide were photodegraded. The relationship between formation ratio of  $\text{NH}_4^+/\text{NO}_3^-$  and chemical structure was also investigated. When the photodegraded intermediate is a primary amine or an amide,  $\text{NH}_4^+$  ion is preferentially produced. On the other hand, when the nitrogen atom in an organic compound is attacked by  $\cdot\text{OH}$  and/or  $\cdot\text{OOH}$  radicals to form a hydroxylamine derivative,  $\text{NO}_3^-$  ions is predominantly produced<sup>5</sup>.

## 6.2 Sulphur-containing surfactants

The sulphonate ( $-\text{SO}_3\text{Na}$ ) in anionic DBS, the sulphonate ( $-\text{OSO}_3\text{Na}$ ) in sodium dodecyl sulphate and the thiocarboxylic salt in TPA (S-dodecylthiopropionic acid salt) can be photomineralized to  $\text{SO}_4^{2-}$  ion via  $\text{SO}_3^-$  ion, but not to form  $\text{H}_2\text{S}$  or  $\text{HS}^-$  derivative. Even if  $\text{S}^{2-}$  ion can be formed, it will change to  $\text{SO}_4^{2-}$  ion immediately by photooxidation<sup>6</sup>. The sulphonate group connected to a benzene ring like DBS can be easily converted to  $\text{SO}_4^{2-}$  ion as shown in figure 6.

Comparing DBS with BS, the formation rate of  $\text{SO}_4^{2-}$  is the same and is not dependent on the alkyl chain length. The hydrophilic sulphonate is adsorbed on  $\text{TiO}_2$  surface more selectively than the hydrophobic alkyl chain. The initial formation rate of  $\text{SO}_4^{2-}$  ion from the decomposition of TPA was relatively slow compared to that of DBS and SDS. With respect to TPA, the decomposition proceeds from the terminal carboxyl group in TPA. The fission of C-S bond and the attack of  $\cdot\text{OH}$  and  $\text{OOH}$  radicals then occur. A polymer such as polystyrene sulphonate can be easily desulphonated.



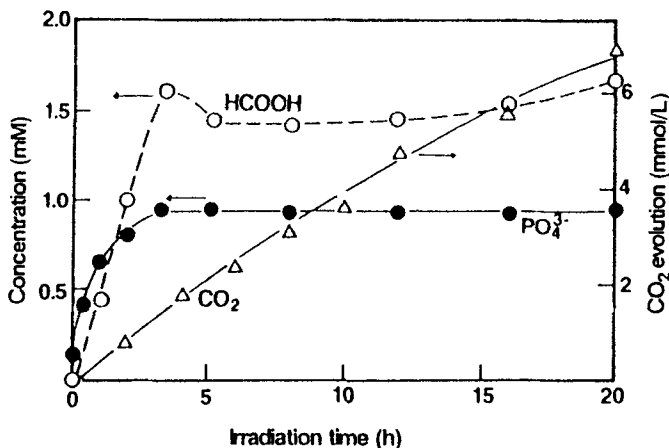


Figure 7. Photodegradation of  $\text{C}_{12}\text{E}_2\text{P}$  in the presence of  $\text{TiO}_2$  catalyst.

### 6.3 Phosphor-containing surfactants

The phosphorous organics employed as agrochemicals are either strongly toxic or carcinogenic. There are few reports on the photodecomposition of phosphor-containing materials. Figure 7 shows the degradation of dodecylbis(oxyethylene) phosphate ( $\text{C}_{12}\text{-EP}$ ). The phosphate group is photomineralized very quickly. In an initial photillumination, it can be converted to  $\text{PO}_4^{3-}$  ion<sup>7</sup>.

### 6.4 Surfactants composed of hydrocarbon

The photodecomposition of a surfactant composed of a long alkyl chain or an ethoxy group gives oxidative intermediates such as peroxides, aldehydes and short carboxylic acid and finally  $\text{CO}_2$  gas is evolved. A nonionic surfactant having a different alkyl chain and oxyethylene group is photodegraded as shown in figures 8(a) and (b). The ethoxyl group is degraded more rapidly than the alkyl group. Preferential  $\text{CO}_2$  evolution is carried out in an initial degradation process. An amount of  $\text{CO}_2$  gas from the degradation of  $\text{C}_{12}\text{E}_m$  ( $m = 5, 6, 7$  and  $8$ ) homologues (1 mmol) is closely related to the number of ethoxyl groups after irradiation of 8 h (see figure 8(a)). Namely, about 10, 12, 14 and 16 mmol of  $\text{CO}_2$  is evolved from  $\text{C}_{12}\text{E}_m$ . The degradation of  $\text{C}_n\text{E}_8$  ( $n = 10, 12, 14, 16$  and  $18$ ) gives the same amount of  $\text{CO}_2$  irrespective of alkyl chain length as shown in figure 8(b). As a result, the oxyethylene group is degraded more easily than the alkyl group and each oxyethylene group is cleaved, one by one, from the terminal<sup>8</sup>.

In order to examine the decomposition of alkyl chain, NMR spectral pattern for the degraded  $\text{D}_2\text{O}$  solution of sodium dodecanoate (10 mM/ $\text{D}_2\text{O}$ ) is illustrated in figure 9.

The terminal methyl proton at 1.14 ppm and the  $\alpha$ -methylene proton at 2.06 ppm are absorbed even after long irradiation time. On the other hand, the signal of alkyl chain at 1.18 ppm decreases when the irradiation time is increased. From the integration of the alkyl chain signal, the dodecyl moiety decreases one methylene group after 2 h-irradiation. Subsequently, the alkyl chain length decreases with irradiation time. The number of ethylene group is four after 10 h-irradiation. The alkyl chain is gradually

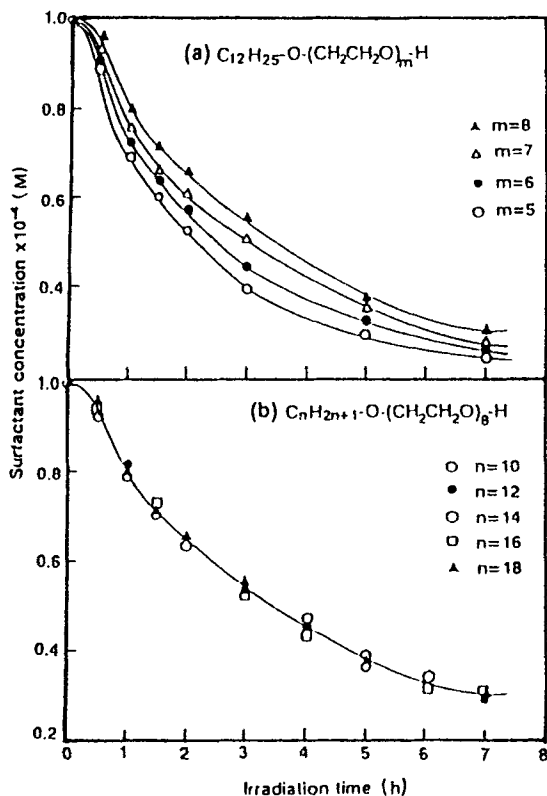


**Figure 8.** Temporal photodecomposition of (a) C<sub>12</sub>E<sub>m</sub> ( $m = 5, 6, 7$  and  $8$ ) and (b) C<sub>n</sub>E<sub>g</sub> ( $n = 10, 12, 14, 16$  and  $18$ ) surfactant solutions (0.1 mM, 50 ml) with TiO<sub>2</sub> (100 mg) monitored by the extraction method

decamped from the terminal position in this way. After irradiation of 30 min, the peak belonging to formyl proton (assigned to aldehyde) is absorbed at a low magnetic field of 8.37 ppm. Further, the signal (1.99 ppm) attributable to acetic acid increases with irradiation time.

## 7. Photoelectrochemical decomposition of surfactants on a TiO<sub>2</sub>/TCO electrode assembly

Promotion of charge separation following irradiation and minimization of electron/hole recombination can occur in a semiconductor film electrode in which TiO<sub>2</sub> particulates are fixed on a transparent conductive oxide (TCO) glass plate. Since the electrons generated by photoexcitation in TiO<sub>2</sub> particles flow to the outlet circuit through a TCO layer, the charge separation is promoted in TiO<sub>2</sub> particles and the recombination is depressed. The colloidal TiO<sub>2</sub> membrane on an electrode surface is so porous that the interesting photochemical and photoelectrochemical characteristics are examined. Recently, the photodecomposition of chloroorganics<sup>9</sup>, dyes<sup>10</sup> and surfactants<sup>11</sup> was carried out. TiO<sub>2</sub> powders (Degussa P-25, anatase) dispersed in aqueous solution were loaded onto a TCO glass plate (Asahi Glass Co. Ltd. transparent

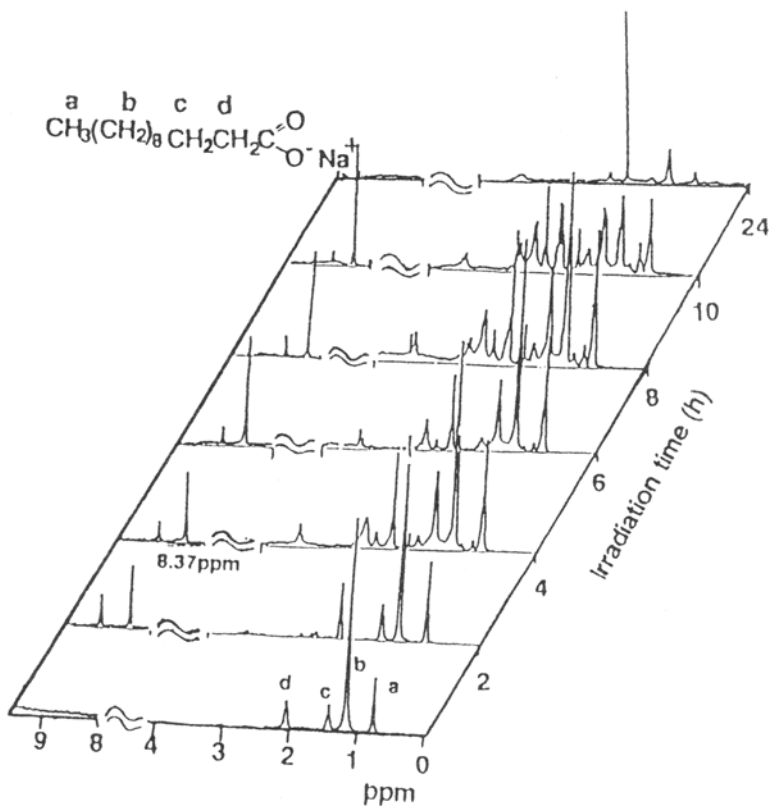


**Figure 9.** Temporal NMR spectral profiles in the photooxidative decomposition of sodium dodecanoate in D<sub>2</sub>O solution (10 mM).

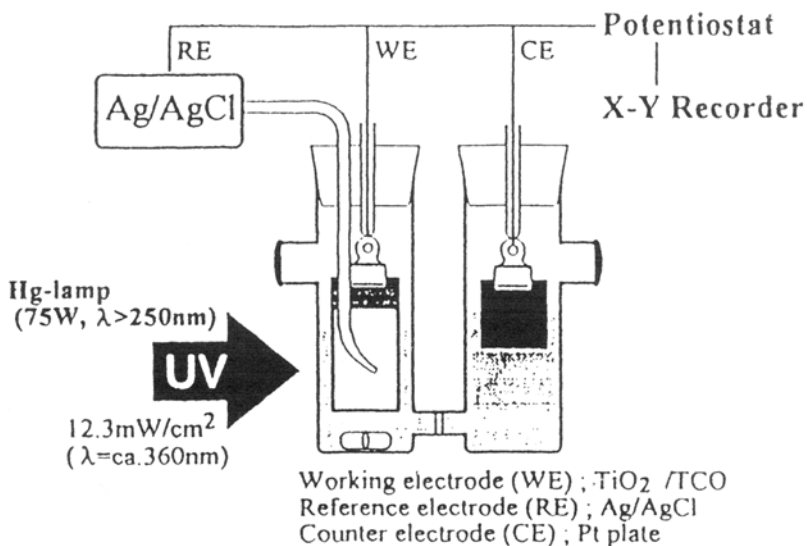


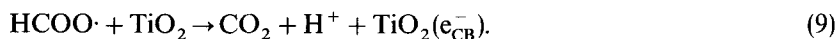
**Figure 10.** Photoreaction cell assembly for potentiometric and voltage-static electrolysis

conductive oxide coated glass plate of fluorine-doped  $\text{SnO}_2$ ) and subsequently dried in air. The plate was sintered for 2 h at  $300^\circ\text{C}$  in a furnace to prepare a particulate film electrode. The TCO coating was  $2.1\ \mu\text{m}$  thick, whereas the thickness of the  $\text{TiO}_2$  thin film was  $4.2\ \mu\text{m}$ . The quantity of  $\text{TiO}_2$  on the area of  $20 \times 30\ \text{mm}^2$  was about 5 mg. The DBS solution ( $0.1\ \text{mM}$ , 50 ml) was contained in a Pyrex glass photoreactor. The anode electrode was a  $\text{TiO}_2/\text{TCO}$  plate and the counter electrode (the cathode) was a Pt plate ( $20 \times 20\ \text{mm}^2$ ); the reference electrode was a Ag/AgCl electrode connected to the assembly via a salt as shown in figure 10.

The photodegradation of a DBS solution at constant applied voltage (5 V) is illustrated in figure 11(a). Addition of supporting electrolytes such as  $\text{Na}_2\text{SO}_4$  or NaCl ( $0.1\ \text{M}$ ) enhances somewhat the photodegradation of the surfactant in comparison with that carried out in an electrolyte-free system. We have reported extensively in earlier reports that the active oxidizing species in photooxidation is the  $\cdot\text{OH}$  radical. The  $\text{CO}_3^{2-}$  ion is a well known  $\cdot\text{OH}$  scavenger and the photooxidation of DBS is therefore expected and is observed to be much slower in carbonate media.

The  $\text{TiO}_2$  electrode potential in the presence of electrolytes stays anodic. As a result, the redox activity of photogenerated electrons and holes should be accelerated. Consequently, the active oxygen species (e.g.,  $\cdot\text{OH}$ ,  $\cdot\text{OOH}$ , and/or  $\cdot\text{O}_2^-$ -radicals) that are likely to oxidize DBS are probably generated in greater quantity. Insofar as the photodegradation of DBS in the presence of  $\text{Na}_2\text{CO}_3$  is concerned, the increase in  $[\text{HO}\cdot]$  from the hydrolysis of the carbonate ion increases the solution pH and consequently renders the  $\text{TiO}_2$  particulate surface negatively charged (the isoelectric point of  $\text{TiO}_2$  is less than pH 6). Under these conditions, adsorption of negatively charged DBS molecules onto the photocatalyst surface is minimized, if not suppressed, and photodegradations should be retarded even further, relative to other electrolytes.

The maximal rate (determined from HPLC experiments having a UV detector),  $k = 2.3 \times 10^{-2}\ \text{min}^{-1}$ , for the photodegradation of DBS is exhibited at an applied potential of  $+0.3\ \text{V}$ . At this applied bias, the photocurrent reached a maximal value immediately after photoreaction and gradually decreased to a constant value (plateau at  $\approx 50\ \mu\text{A}$ ) at 2 h of irradiation time (figure 11(b)). We attribute the maximal photocurrent to the oxidation of formic acid which was the principal intermediate product before  $\text{CO}_2$  evolution. Electrons that appear in the conduction band of  $\text{TiO}_2$  and lead to increased photocurrent, originate from reactions 8 and 9



The photocurrent flows through the external circuit. The "current doubling" phenomenon reported by others evidently also takes place in the photooxidation process of the DBS surfactant.

The behaviour of the photogenerated current as a function of irradiation time at a bias of  $-0.3\ \text{V}$  fluctuates between anionic and cationic levels. The current was rather small compared with that at other applied potential bias. This potential of  $-0.3\ \text{V}$  refers to the zero current potential and corresponds approximately to the flat band potential of the conduction band of  $\text{TiO}_2$  under the prevailing conditions. The stagnant electrons in the bulk of  $\text{TiO}_2$  are deactivated by recombination with the valence band holes. Thus, the reactivity was lower and formation of active oxygen species was suppressed leading to a decrease in the rate of degradation of DBS. At a  $-0.5\ \text{V}$  bias,

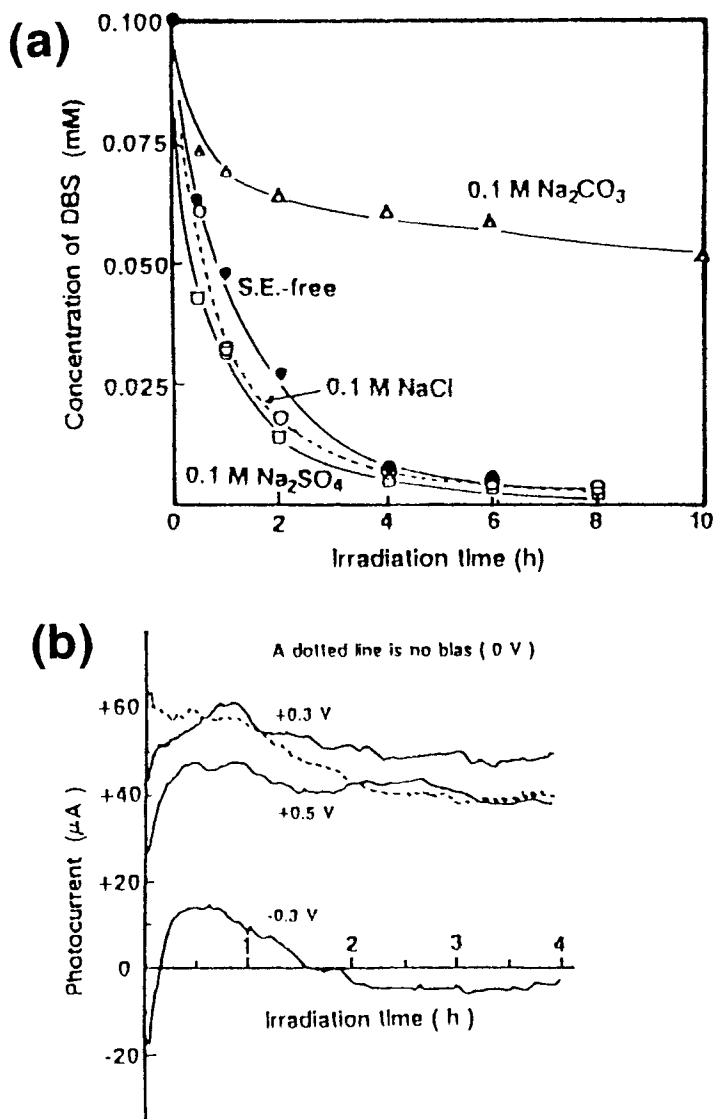


**Figure 11.** (a) Temporal changes in the concentration of DBS (0.1 mM) in a photoelectrochemical  $\text{TiO}_2/\text{TCO}$  cell assembly in various electrolyte (0.1 M) systems at a constant bias of 5 V. S.E. stands for a supporting electrolyte. (b) Photocurrent generated in a  $\text{TiO}_2/\text{TCO}$  electrode assembly during the photodegradation of DBS by a potentiostatic electrolysis.

any accumulation of electrons at the  $\text{TiO}_2$ /solution interface enhances the reduction of  $\text{O}_2$  and/or  $\text{H}^+$ , such that the largest quantity of electricity (in terms of number of coulombs) based on a cathodic current was measured at this bias. On the other hand, the holes formed by charge separation are diffused to the bulk of  $\text{TiO}_2$  particulates and formation of  $\cdot\text{HO}$  radicals is thereby limited. Consequently, the rate of photodegradation of DBS decreased.

Applied voltages were from a DC potentiostat and the UV illumination was provided by a Toshiba mercury lamp. The potentials at the TiO<sub>2</sub> electrode were measured with an electrometer. The temporal changes in the concentrations of the photodegraded DBS surfactant were monitored by high performance liquid chromatography (HPLC) using UV-detection. Figure 10 illustrates the photoelectrolysis setups for potentiometric and photocurrent measurements, respectively. The latter measurements were carried out using a potential step method with a potentiogalvanostat. The temporal disappearance of DBS was also undertaken electrolytically using a pair of Pt electrodes (as anode and cathode).

### Acknowledgements

This research was supported by a grant-in aid for Scientific Research from the Ministry of Education (No. 06640757) and by the Environmental Protection Project Foundation from the Ministry of Public Health. The authors also appreciate the Cosmetology Research Foundation for financial support.

### References

1. Hidaka H, Zhao J, Pelizzetti E and Serpone N 1992 *J. Phys. Chem.* **96** 2226
2. Gerischer H and Heller A 1991 *J. Phys. Chem.* **95** 5261
3. Low G K-C, Mc Evoy S R and Matthews R W 1991 *Environ. Sci. Technol.* **25** 460
4. Hidaka H, Nohara K, Zhao J, Pelizzetti E and Serpone N 1995 *J. Photochem. Photobiol. A: Chem* **91** 145
5. Hidaka H, Nohara K, Zhao J, Pelizzetti E and Serpone N, Guillard C and Pichat P 1996 *J. Adv. Oxidation Tech.* **1** 21
6. Hidaka H, Nohara K, Ooishi K, Zhao J, Pelizzetti E and Serpone N 1994 *Chemosphere* **29** 2619
7. Hidaka H, Zhao J, Satoh Y, Nohara K, Pelizzetti E and Serpone N 1994 *J. Mol. Catal.* **88** 239
8. Hidaka H, Zhao J, Kitamura K, Nohara K, Pelizzetti E and Serpone N 1992 *J. Photochem. Photobiol. A: Chem.* **64** 103
9. Liu D and Kamat P V 1993 *J. Phys. Chem.* **97** 10769
10. Vinodgopal K and Kamat P V 1995 *Environ. Sci. Technol.* **29** 841
11. Hidaka H, Asai Y, Zhao J, Nohara K, Pelizzetti E and Serpone N 1995 *J. Phys. Chem.* **99** 8244